Check for updates

Estimation of evaporation from saline water

Seyed Mostafa Biazar • Ahmad Fakheri Fard • Vijay P. Singh • Yagob Dinpashoh • Abolfazl Majnooni-Heris

Received: 1 March 2020 / Accepted: 24 September 2020 © Springer Nature Switzerland AG 2020

Abstract Evaporation, as the main source of water loss from closed lakes, makes a significant contribution to the water balance equation of the lake and can lead to changes in the chemical composition thereof. The objective of the study was to develop an equation for estimation of evaporation from the water surface with different depths and concentrations. To that end, 48 barrels were used to model evaporation at 6 different depths and 8 different concentrations of salinity. The experiments have been conducted in the same meteorological condition for all the barrels near the Urmia Lake. Data were collected in March 1, 2019, to Aug 31, 2019. Different equations fitted to data for each concentrations of salinity separately with different depths, and the equations with the least errors were selected. A model

S. M. Biazar () · A. F. Fard · Y. Dinpashoh · A. Majnooni-Heris
Department of Water Engineering, Faculty of Agriculture, University of Tabriz, Tabriz, Iran
e-mail: Seyedmostafa.b@gmail.com

e-mail: SM.Biazar@tabrizu.ac.ir

Published online: 10 October 2020

V. P. Singh

Caroline & William N. Lehrer Distinguished Chair in Water Engineering, Department of Biological and Agricultural Engineering, Texas A&M University, 321 Scoates Hall, 2117 TAMU, College Station, TX 77843-2117, USA e-mail: vsingh@tamu.edu

V. P. Singh

Zachry Department of Civil & Environmental Engineering, Texas A&M University, 321 Scoates Hall, 2117 TAMU, College Station, TX 77843-2117, USA

was then developed for the estimation of evaporation, considering the effect of salinity and depth, and the results were compared with daily measurements. The results were evaluated using the root mean square error (RMSE), correlation coefficient (CC), and Nash-Sutcliffe efficiency coefficient (NS). The results indicated that evaporation (Horizontal row) from water surface with high concentrations of salinity to low concentrations of salinity in different depths had an incremental trend. However, it can be seen in the vertical row that evaporation increased from low depth to high depth, and then decreased at a certain depth (120 cm) while the maximum evaporation rate belonged to 90-cm barrels for each concentration of salinity (in the vertical and horizontal row). At the end, the comparison of evaporation computed from the model and measured data showed that the model estimated evaporation at different depths and concentrations of salinity satisfactorily.

Keywords Evaporation · Equation · Different depth · Different Concentration · Saline water

Introduction

Many of the world's saline lakes are shrinking, with the result that bird habitats are being undermined, people living around the lake are suffering from economic losses, and dusty winds are increasing which are threatening people's health (Wurtsbaugh et al. 2017; Dinpashoh et al. 2019; Khaledian et al. 2020; Biazar et al. 2020a).



Observations have shown that a significant portion of lake water in arid and semiarid areas is lost through evaporation, and evaporation from water bodies strongly depends on surface water salinity (Biazar et al. 2019; Mor et al. 2018). Direct measurement of evaporation is expensive, cumbersome, and has different sources of error, and becomes even more difficult for evaporation from saline water with different concentrations of salinity. Climatic parameters, influencing saline water evaporation, not only vary from station to station but also vary based on the degree of salinity (Asmar and Ergenzinger 1999; Mor et al. 2018; Hamdani et al. 2018). The rate of evaporation from saline water surface is usually less than that from fresh water (Asmar and Ergenzinger 1999). Therefore, different models have been derived for saline water evaporation. Although mainly studied at the pan evaporation scale, the effect of surface water salinity on evaporation has not yet been investigated by means of direct measurement at the scale of natural water bodies (Mor et al. 2018).

Many investigators have estimated evaporation from lake water surfaces (Gianniou and Antonopoulos 2007). The mechanics of evaporation from saline water are somewhat different from those from fresh water. The complexity of the process of evaporation from water bodies (e.g., lakes, ponds, dams, and natural reservoirs) and the lack of sufficient and reliable measured data have been the main obstacles (Lin and Sandler 1999; Hamdani et al. 2018).

Lee (1927) compared evaporation from pure water and from Brine Lake in Nevada, USA, for different water densities and found that brine water evaporation in comparison with pure water reduced by 0.01% for a 1% increase in the specific weight of water. Young (1947) compared evaporation from saline water (with different concentrations of sodium chloride) and that from fresh water, and their results did not significantly differ from the findings of Lee (1927). Kokya and Kokya (2008) analyzed the effect of salinity of water on evaporation rate from a water pan in an experimental study near the Urmia Lake. They proposed a formula for evaporation measurement from salt water. Results are compared with Meyer and Harbeck methods. The results showed that have been proposed methods could estimate evaporation with higher accuracy than classical methods. AL-Khlaifat (2008) reported that the average volume of evaporation loss from the Dead Sea was between 2 and 4 billion m³/ year during 1800-2000. He also showed that the decrease in lake level over time had resulted in reduced evaporation. Furthermore, the evaporation rate had decreased due to increased salinity with significantly lower lake water level. Kisi et al. (2015) predicted the Urmia Lake water level with the support vector machine (SVM) model, and compared the output of the SVM-firefly algorithm (FA) model with that of genetic programming (GP) and artificial neural networks (ANNs) models, and showed that the SVM-FA model was superior to others. Shiri et al. (2016) predicted the water level in the Urmia Lake using the extreme learning machine (ELM) method and compared it with ANN and GP and found the ELM method to be better. Ma et al. 2016 conducted a research about evaporation variability of Nam Co Lake in the Tibetan Plateau and its role in recent rapid lake expansion. At this study, evaporation of Nam Co Lake was investigated within the 1979-2012 period at a monthly time-scale using the complementary relationship lake evaporation model which does not require wind speed data. Validations by in situ observations of E601B pan evaporation rates at the shore of Nam Co Lake as well as measured evaporation over an adjacent small lake using eddy covariance technique suggested that complementary relationship lake evaporation is capable of simulating evaporation well since it implicitly considered wind effects on evaporation via its vapor transfer coefficient. Hamdani et al. (2018) assessed seasonal and daily evaporation of the deep and brine Dead Sea. They found that the peak evaporation rate occurring in summer was related to solar radiation, and the winter peak evaporation was related to the thermal storage of the lake and high vapor pressure combined with wind and resulted in thermal instability. They compared several models of evaporation with direct measurements, and showed that the mass transfer model was more reliable than the others. Mor et al. (2018) investigated the effect of water surface salinity on evaporation in case of diluted buoyant plume over the Dead Sea. They measured surface heat fluxes, micrometeorological variables, and water temperature and salinity profiles, simultaneously and directly over the salty lake, and over a region of diluted buoyant plume. The results showed that the evaporation rate from the diluted plume was occasionally 3 times larger than that of the main salty lake. In the open lake, where salinity was uniform with depth, increased wind speed resulted in increased evaporation rate. However, in the buoyant plume where diluted brine floats over the hyper saline brine, wind speed above a threshold value (~ 4 m s⁻¹)



Environ Monit Assess (2020) 192:694 Page 3 of 17 694

caused a sharp decrease in evaporation probably due to mixing the stratified plume with a consequent increase in the surface water salinity. Wang et al. 2018 carried out a research about global lake evaporation accelerated by changes in surface energy allocation in a warmer climate. Here, they reported simulations with a numerical model of lake surface fluxes, with input data based on a high-emission climate change scenario (Representative concentration of salinity Pathway 8.5). In their simulations, the global annual lake evaporation increased by 16% by the end of the century, despite little change in incoming solar radiation at the surface. Nozari and Azadi (2019) predicted the salinity of drainage and groundwater at various drain depths and spaces and showed that ANN had a reasonable accuracy in the simulation of temporal shallow groundwater and drainage of water salinities at different drain depths and drain spaces. Vaheddoost and Kocak (2019) have investigated temporal dynamics of monthly evaporation in Lake Urmia using chaos theory. Since evaporation at each station was measured by means of class A evaporation pan, time series at each station was multiplied by a pan coefficient to incorporate the effect of saline water and free water surface environment simultaneously. Measurement errors arising from assumption of zero evaporation in winter were removed from the time series using locally weighted scatterplot smoothing method after which the unification of time series into a single time series was achieved. Results of the data transformation and information loss were monitored by means of auto-correlation, partial-auto-correlation, mutual information, power spectrum, false nearest neighbor, and correlation dimension. A local prediction method was then used to capture the temporal dynamics of the evaporation with consideration of an appropriate time delay and embedding dimension. Finally, the representative model was projected on a 3-dimensional phase space to evaluate the temporal dynamics of the evaporation. Results indicated that the chaotic approach showed accurate predictions in advance. Guo et al. (2019) conducted a research on long-term changes in evaporation over Siling Co Lake on the Tibetan Plateau and its impact on recent rapid lake expansion. In this study, long-term evaporation over Lake Siling Co was simulated using a singlelayer lake evaporation model, and the simulated result was verified by observation from an eddy covariance system in the lake. The results showed that the singlelayer lake evaporation model was capable of accurately simulating the lake evaporation on a daily scale.

The main objective of this study therefore was to develop an equation for estimating evaporation from saline water with different depths and concentrations of salinity.

Materials and methods

Study area

Lake Urmia is one of the most significant saline lakes of the world and Iran's largest saline lake, which is at risk of drying up because of excessive agricultural development, climate change, and irrational construction of dams. Various reports have been presented regarding evaporation from the lake surface, with the values generally estimated to be in the range of 890 to 1360 mm per year (more than 50% difference). However, just 1 cm of error in estimating the evaporation height leads to 30 million cubic meters of error in calculating the lake water balance, considering the average lake area of 3000 k². This shows the necessity of accurately estimating the evaporation rate from Lake Urmia using physically based approaches and accurate observed data.

Method and experiments

First, a place closest to Lake Urmia where a station could be built was selected for the study. Then, the station was equipped (Fig. 1). Plastic barrels of different heights were prepared, and waters with different concentrations of salinity were monitored to measure the evaporation. Urmia lake salt and distilled water were used for conducting this experiment because the distilled water concentration of salinity has been known, and it was possible to easily control the concentration of salinity of barrels with electrical conductivity meter. The water level in all barrels was kept near the barrel surface. A separate scale was prepared for each barrel, and the numbers on them were read every day. Distilled water was added to the barrels every few days to reach the initial level of water and salinity (El-Dessouky et al. 2002; Lide 2005). After adding water to the barrels, they were stirred with separate plastic tubes designed for each barrel, and then the tubes were washed using distilled water and the water used to wash them was poured into the barrels again, because it was intended to control the barrel concentrations of salinity (On the days



594 Page 4 of 17 Environ Monit Assess (2020) 192:694



Fig. 1 Study area, (a) barrels, (b) thermometer, (c) weighbridge) to measure the salt weight of the barrels), (d) scale (to measure the water sample), (e) electrical conductivity (EC), total dissolved solids (TDS) meter (f) on the left-hand side; rain gauge and on

the right-hand side; meteorological parameters measuring devices) wind speed, air temperature, air humidity, barometer, sunshine hours, etc.) and (g) geographical coordinates of study area

when distilled water was added to the barrels, the scales were read once before adding the water and once after adding the water and stirring).

Measurements at a daily scale were made for the evaporation rate of saline water with different concentration of salinity levels. Forty-eight different samples (with salt and water) were made with different concentrations of salinity and different depths. The sample concentrations of salinity were 0.2 g/l (as a fresh water), 5 gr/l, 10 g/l, 20 g/l, 50 g/l, 100 g/l, 300 g/l, and 500 g/l, exposed to free evaporation in the field. The sample depths were 10 cm, 25 cm, 50 cm, 75 cm, 90 cm, and 120 cm.



Environ Monit Assess (2020) 192:694 Page 5 of 17 694





Fig. 1 (continued)

Data

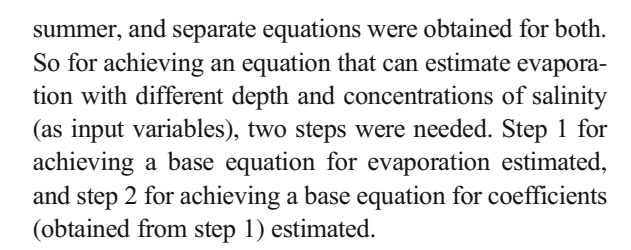
The barrels were arranged in two rows of vertical and horizontal. In the horizontal row, there were 8 barrels, and in the vertical row, there were 6 barrels. In the horizontal row, the depth was constant and the concentration of salinity was varied, while in the vertical row, the concentration of salinity was constant and the depth was varied. The evaporation rate was measured daily from March 1, 2019, to Aug 31, 2019. In order to keep the water surface clear from algae and other thin films, the water surface was cleaned from time to time, since any dust precipitation over the water surface would retard evaporation (El-Dessouky et al. 2002). The data were divided into two parts: winter and spring and summer, because the winter evaporation rate was very different from spring and summer.

Modeling

The observed data was analyzed using MATLAB software and its applications and curve fitting option, and different equations were fitted to the data in two steps as follows.

Step 1: In order to derive an evaporation equation, evaporation data were used for various depths and concentrations. Depth and concentrations of salinity were used as input variables and evaporation as an output variable. Different equations (Interpolant, Exponential, Fourier, Gaussian, Linear fitting, Polynomial, Power, Rational, Smoothing Spline, Sum of sine, Weibull, etc.) were fitted to data for each concentration of salinity separately with different depths, and the equations with the least errors were selected. It was noted that for the same evaporation rate, the same model had different parameters (coefficients) for different concentrations of salinity (each model had different parameters or coefficients) so it was needed to carry out step 2.

Step 2: To derive a general equation, parameters (the coefficients that obtained in the step 1) of the selected model were reinvestigated and by fitting different equations (Interpolant, Exponential, Fourier, Gaussian, Linear fitting, Polynomial, Power, Rational, Smoothing Spline, Sum of sine, Weibull, etc.) to the values of parameters (coefficients) obtained in the previous step (step 1), an optimal parameter set for the final model (equation) was obtained (by trial and error). These steps were used for the first two steps of winter and spring and



Model performance

Three metrics were applied to assess model performance, including the (i) coefficient of correlation (CC), (ii) root mean square error (RMSE), and (iii) Nash-Sutcliffe model efficiency coefficient (NS) (Nash and Sutcliffe 1970; Isazadeh et al. 2017; Ashrafzadeh et al. 2018; Deo et al. 2018; Aghelpour et al. 2019):

$$CC = \sqrt{\frac{\left(\sum\limits_{i=1}^{N} \left(x_i - \overline{x}\right) \left(y_i - \overline{y}\right)^2\right)}{\left(\sum\limits_{i=1}^{N} \left(x_i - \overline{x}\right)^2 \sum\limits_{i=1}^{N} \left(y_i - \overline{y}\right)^2\right)}}$$
(1)

$$RMSE = \sqrt{\frac{\left(\sum\limits_{i=1}^{N} \left(x_i - \overline{y}\right)^2\right)}{N}}$$
 (2)

$$NS = 1 - \sqrt{\frac{\left(\sum\limits_{i=1}^{N} \left(x_i - \overline{y}\right)^2\right)}{\left(\sum\limits_{i=1}^{N} \left(x_i - \overline{x}\right)^2\right)}}$$
(3)

where x_i is the i-th observed value, \overline{x} is the mean of observations, y_i is the i-th value estimated from the model, \overline{y} is the mean of the estimated values, and N is the number of observations (Naganna et al. 2019; Ashrafzadeh et al. 2019; Ashrafzadeh et al. 2020; Biazar et al. 2020b).

Results

Step 1

Tables 1 and 2 indicate the best fitted equations given for the observed data (step 1). In these tables, the



Environ Monit Assess (2020) 192:694 Page 7 of 17 694

Table 1 Evaporation equations for saline water with different depths and concentration of salinity in winter period

Concentration (g/l)	Equations	a_1	b_1	c_1	a_2	b_2	c_2	RMSE
Fresh water		0.664	88.39	23.22	1.667	98.44	165.1	0.02118
5	$f(x) = a_1 \cdot \exp\left(-\left(\frac{(x-b_1)}{c_1}\right)\right)^2 + a_2 \cdot \exp\left(-\left(\frac{(x-b_2)}{c_2}\right)\right)^2$	1.091	82.4	40.48	1.767	1149	1604	0.06047
10		1.103	84.01	45.49	1.208	- 228	759.6	0.1051
20		0.5717	88.48	18.12	1.501	80.58	111.7	0.03053
50		0.36	92.55	13.5	1.715	96.07	132.8	0.04433
100		0.3489	92.05	11.49	1.746	103	135.1	0.06888
300		0.3845	91.1	12.01	1.5	82.79	118.1	0.06707
500		0.5495	90.35	15.1	1.185	70.72	115	0.05596

(x is the depth value)

equation was observed for each concentration of salinity. However, the equations were the same for all concentrations of salinity, but the coefficients of equations were different. As mentioned before, the equations for the two periods of winter and summer and spring, which were continuously measured, were obtained. Therefore, the equation selected was

$$f(x) = a_1 \cdot \exp\left(-\left(\frac{(x-b_1)}{c_1}\right)\right)^2 + a_2 \cdot \exp\left(-\left(\frac{(x-b_2)}{c_2}\right)\right)^2$$

$$(4)$$

where f(x) is a function (evaporation value that will be estimated); x is the depth value (10 cm, 25 cm, 50 cm, 75 cm, 90 cm, and 120 cm); and a_1 , b_1 , c_1 , a_2 , b_2 , and c_2 are the coefficients obtained from step 1.

Step 2

Tables 3 and 4 show the equations for estimating the coefficients of Eq. 4 of Tables 1 and 2 (step 1). As in Tables 1 and 2, all the coefficients were used for the same equation which differed only in the coefficients. In this section, a trial and error method was used for selecting the optimal coefficients for the original equation that the domain of coefficients of variation and their optimal values have been presented for different concentrations of salinity in Tables 3 and 4. Equation (5) was selected as the coefficient equation:

$$Z(t) = (p_1.t^3 + p_2.t^2 + p_3.t + p_4)/(t^2 + q_1.t + q_2)$$
(5)

where Z(t) is a function (coefficient value that will be estimated); t is the concentration of salinity value (fresh water, 5 (g/l), 10 (g/l), 20 (g/l), 50 (g/l), 100 (g/l), 300 (g/l),

Table 2 Evaporation equations for saline water with different depths and concentration of salinity in spring-summer period

Concentration (g/l)	Equations	a_1	b_1	c_1	a_2	b_2	c_2	RMSE (mm/ day)
Fresh water		1.751	94.71	15.71	10.92	88.2	139.6	0.1942
5	$f(x) = a_1 \cdot \exp\left(-\left(\frac{(x-b_1)}{c_1}\right)\right)^2 + a_2 \cdot \exp\left(-\left(\frac{(x-b_2)}{c_2}\right)\right)$	1.589	90.91	15.18	10.62	92.09	149.6	0.1831
10	2	1.692	89.06	15.67	10.3	95.02	156.2	0.174
20		1.715	89.67	14.86	10.11	96.02	158.4	0.1577
50		1.473	90.19	14.58	9.958	97.77	158.7	0.215
100		1.461	91.02	13.62	9.579	95.99	155.3	0.211
300		2.687	84.05	34.92	9.50E + 00	9.40E+01	152	0.2616
500		2.284	84.85	34.24	9.45	90	148	0.2223

(x is the depth value)



 Table 3
 The equation coefficients for winter period

Coefficients Equation		p_1		p_2		p_3		p_4		q_1		q_2	
		Value	Range	Value Range	Range	Value	Range	Value Range	Range	Value	Value Range	Value Range	Range
a_1	$Z(t) = (p_1, t^3 + p_2, t^2 + p_3, 0.000573* (0.0001005, t + p_4)/(t^2 + q_1, t + q_2)$ 0.001045	0.000573*	(0.0001005, 0.001045)	0.2315	0.2315 (0.05885, 0.5887 (-6.942, 3.00E (2.838, 0.4041) 8.119) + 01 57.16)	0.5887	(-6.942, 8.119)	3.00E + 01	(2.838, 57.16)	- 11-	(-17.16, - 66.98 (34.97, 11. 5.42) 99)	86.98	(34.97, 99)
b_1		- 0.00737	00737 (- 0.01942, 0.004672)	94.01	(89.28, 98.74)	- 636.7 (- 2367, 1093)	(-2367, 1093)	3894	3894 (-2810, 1.06e+ 04)		(– 26.66, 14.8)	41.76	41.76 (-35.68, 119.2)
c_1		0.007639	(-0.008477, 0.02375)	10.47	10.47 (4.889, 16.05)	– 1.06E + 02	-1.06E (-284.2, 1.24E (504.7, +02 72.4) +03 1969)	1.24E + 03	(504.7, 1969)	⁶ - 45	(-17.17, -7.08E (47.46, 11.57) + 01 94.11)	7.08E + 01	(47.46, 94.11)
a_2		-0.00203	(-0.004699, 0.0006473)	2.156	2.156 (1.136, 3.176)	101.4	101.4 (-403.9, -1005 (-5433, 606.8) 3422)	- 1005	(– 5433, 3422)	71.87	57 71.87 (-258.7, 402.4)	- 63-	(-3344, 2078)
b_2		- 0.07858	(-0.1339, -0.02322)	110.7	(91.62, 129.8)	- 1736	- 1736 (- 2074, - 4853 1398)	4853	(4349, 5357) –	13-	(-15.13, - 11.83)	5.4 41.48	(32.16, 50.81)
C_2		- 0.05772	(-0.1173, 0.001844)	142.6	(122.6, 162.5)	- 2453	(- 2982, - 1923)	8.50E + 03	- 2453 (- 2982, - 8.50E (7236, 9768) 1923) + 03	.48 - 15- .46	(- 15.96, - 14.95)	52.15	(50.25, 54.05)

*This value will be changed for 300 and 500 (g/l) concentration of salinity to 0.000473

~
perio
spring-summer
for
coefficients
Equation
able 4

			'										
Coefficients	Coefficients Equation	p_1		p_2		p_3		p_4		q_1		q_2	
		Value	Range	Value	Range	Value	Range	Value	Range	Value	Value Range	Value	Range
a_1	$Z(t) = (p_1, t^3 + p_2, 0.00045 (-1.000045) (-1.000000000000000000000000000000000000$	0.00045	(- 0.00125- 9, 0.00215- 8)	1.754	1.754 (0.656, 2.853)	- 43- 0.1	(- 602.3, - 257.9)	1.36E + 04	(-1.01e + 04, 3.737e + 04)	- 25- 9.4	(-351.3, 8144 (-5318, - 2.1610 167.4) 04)	8144	(-5318, 2.161e + 04)
b_1		- 0.01- 53	5125, 2066)	91.4	(78.53, 104.3)	- 77- 1.8	(-8025, 6481) 2590	2590	(-1.87e + 04, 2.388e + 04)	8	(- 92.73, 27.41 76.23)	27.41	(– 184.5, 239.3)
c_1		25.65	(– 40.9, 92.19)	- 89- 24	(-4.779e + 04, 2.994e + 04)	1.12E + 06	(-7.669e + 06, 9.904e + 06)	- 7.79E- +06	(-1.286e + 08, 1.13e + 08)	- 46- 1.2	(– 3193, 2270)	7.07E + 04	(-5.101e + 05, 6.515e + 05)
a_2		- 0.00- 022	(- 0.00251- 5, 0.00207-	9.507*	9.507* (8.509, 10.5)		36.21* (- 703.2, 775.6)	-1554	(- 6225, 3118) 1.629 (- 70.79, 74.05)	1.629	(– 70.79, 74.05)	- 13- 9.7	(– 563.5, 284.1)
b_2		- 0.01- 781	(-0.02935, 99.33 -0.00625-		(94.89, 103.8)	- 10- 17	(-7095, 5061) - 3506	-3506	(-1.787e + 04, 1.086e + 04)	- 9 1	(– 71.34, 52.02)	- 43 01	(- 216.8, 130.8)
c_2		- 0.01- 488	(-0.04556, 0.0158)	154.7	(135.8, 173.6) 3803		(- 2.473e + 04, 3.234e + 04)	1.21E + 04	(-3.851e + 04, 6.279e + 04)	22.35	22.35 (-150.3, 97.17 (-324.1, 195) 518.5)	97.17	(- 324.1, 518.5)

*These values will be changed as below for 300 and 500 (g/l) concentration of salinity as below. $P_2 = 8.509$ and $P_3 = -703.2$

694 Page 10 of 17 Environ Monit Assess (2020) 192:694

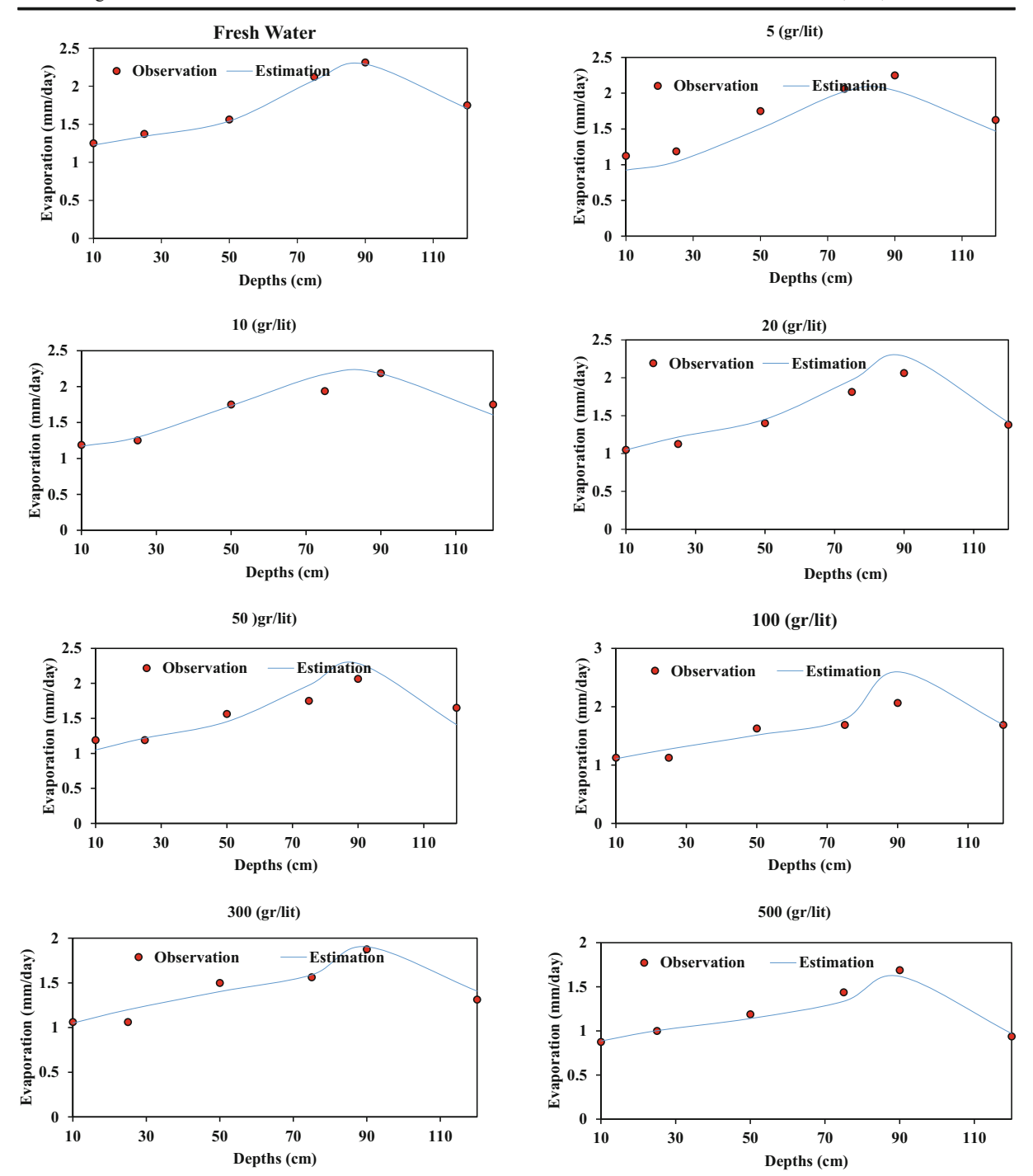


Fig. 2 Comparison of observational and computational values for all depths and concentrations of salinity (winter period)

and 500 (g/l)); a_1 , b_1 , c_1 , a_2 , b_2 , and c_2 are the coefficients for the last equation (Eq. 4); and p_1 , p_2 , p_3 , p_4 , q_1 , and q_2 are the coefficients obtained from step 2.

Computational and observation graphs have been compared in Figs. 2 and 3. As can be seen, the proposed

equation was able to estimate the value of evaporation at different concentrations of salinity and depths. Table 5 also shows that the present equation estimated evaporation from saline water well for all depths and each separate concentration. Further, Figs. 2 and 3 reveal that



Environ Monit Assess (2020) 192:694 Page 11 of 17 694

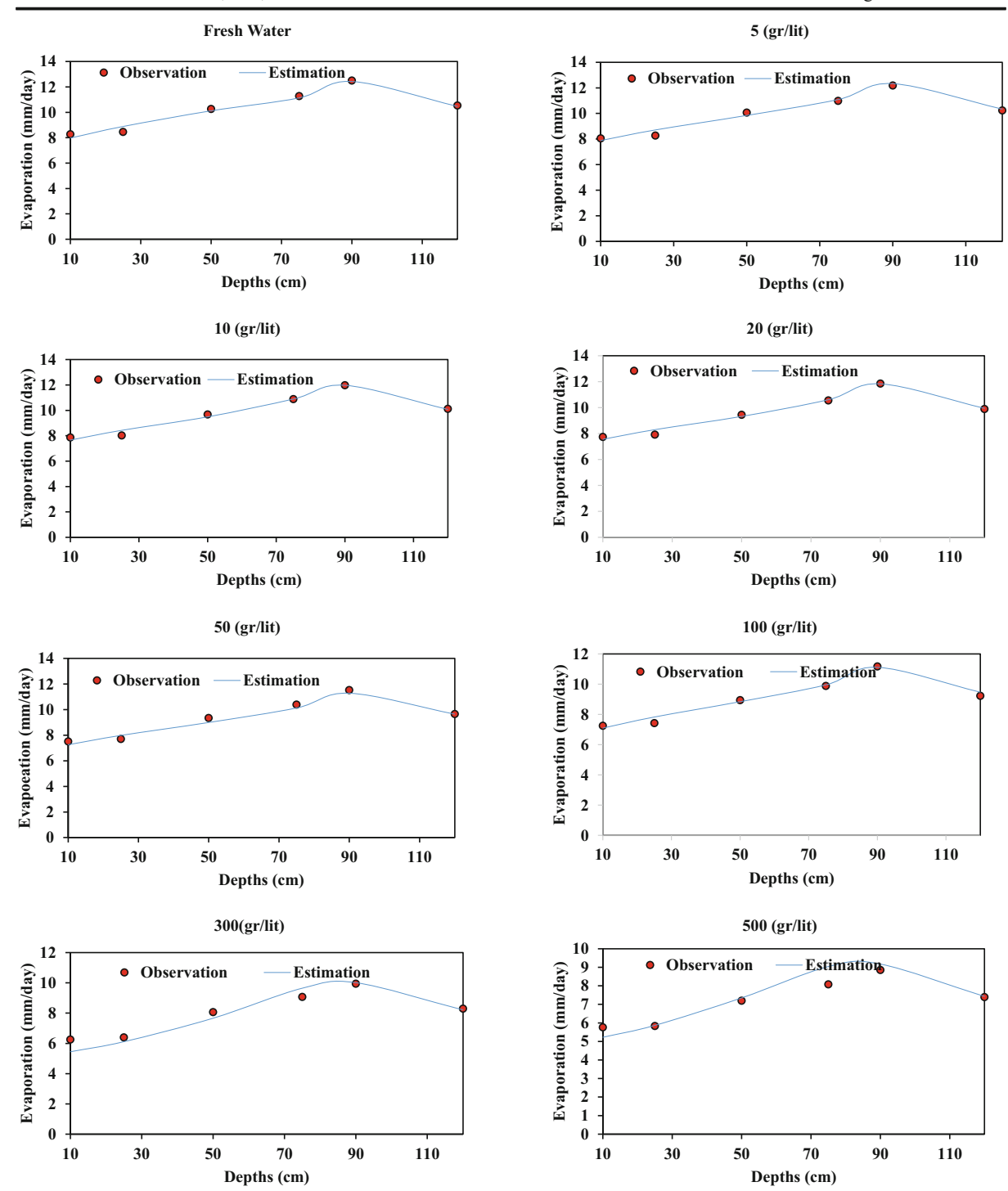


Fig. 3 Comparison of observational and computational values for all depths and concentrations of salinity (spring-summer period)

the maximum evaporation value had occurred in summer (Hamdani et al. 2018). However, the 90-cm barrels had the maximum evaporation rate during the entire recording period.

According to the results, it can be seen that the evaporation from the water with high concentration of salinity is increasing toward low concentration of salinity (Figs. 4 and 5). The evaporation also increases from



694 Page 12 of 17 Environ Monit Assess (2020) 192:694

Table 5 Average modeling results of all depths and concentration of salinity

Period	Concentration (g/l)	RMSE	NS	CC
Spring-Summer	Fresh water	0.235	0.975	0.988
	5	0.226	0.976	0.989
	10	0.201	0.981	0.978
	20	0.183	0.983	0.992
	50	0.254	0.968	0.989
	100	0.210	0.976	0.989
	300	0.456	0.882	0.985
	500	0.470	0.824	0.977
Winter	Fresh water	0.033	0.993	0.987
	5	0.179	0.813	0.948
	10	0.114	0.897	0.957
	20	0.121	0.887	0.996
	50	0.130	0.890	0.996
	100	0.235	0.903	0.930
	300	0.081	0.921	0.965
	500	0.056	0.963	0.995

low (10 and 25 cm) to high depths (50, 75, and 90 cm) and then decreases again at specific depths (120 cm) (Fig. 6). During the winter measurement period, water is

sometimes disturbed due to freezing at low concentrations.

According to Tables 6 and 8, the water surface temperature has an upward trend from barrels with high depth to less depth and from low to high concentration of salinity. That is, the higher concentration of salinity leads to an increase of more water surface temperature in barrels with the same height, and if we consider the concentration of salinity to be the same, the lower height of the barrel leads to an increase of more water surface temperature than the high barrel. The bottom water temperature shows an upward trend from high to lower depth barrels and from low to high concentration of salinity (Tables 7 and 9). The measurement of water temperature shows that water temperature generally decreases from the surface to the bottom (except for 25-and 10-cm barrels).

The amount of evaporation of saline water will be reduced. Still, the mechanism is the same because the molecules-cations interaction will be more significant, and this will reduce the evaporation rate in saline water. Also, layering is done with high concentration of salinity in saline, and the lower part will have the highest possible concentration of salinity in which the release of water molecules will be

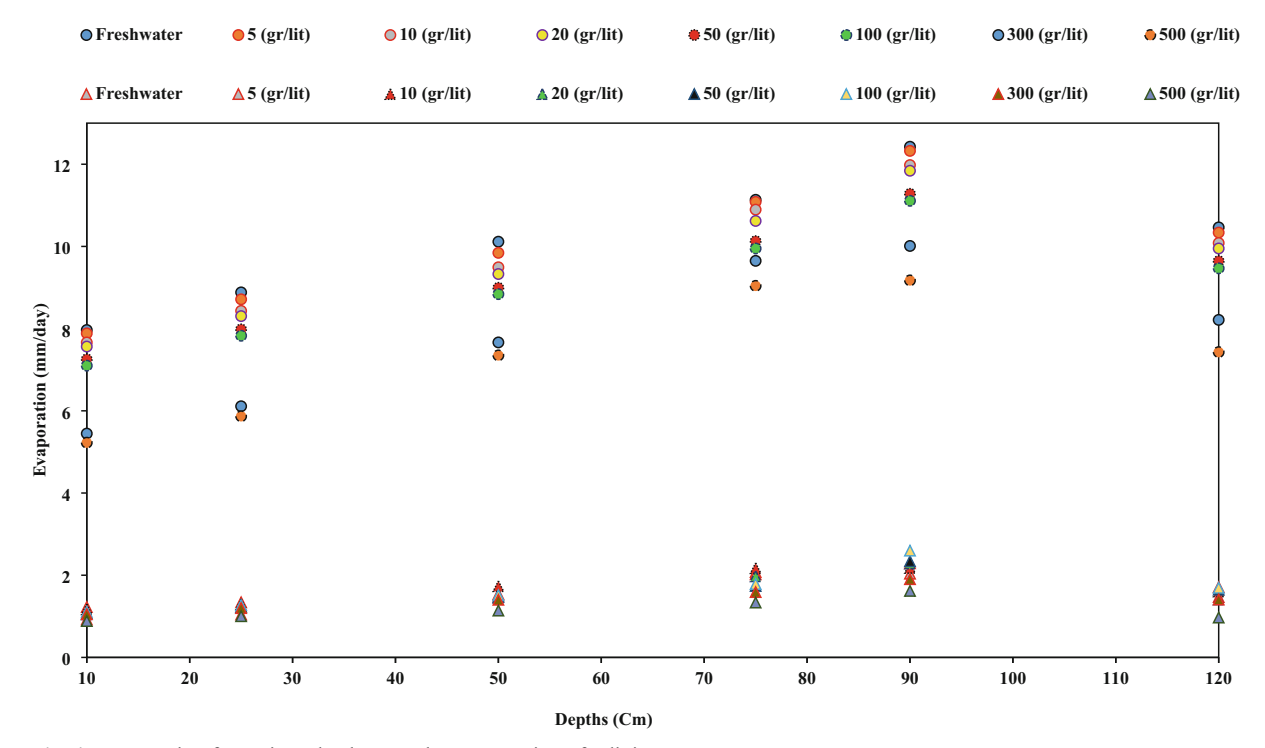


Fig. 4 Evaporation for various depths at each concentration of salinity



Environ Monit Assess (2020) 192:694 Page 13 of 17 694

010 (Cm) 025 (Cm) 050 (Cm) 075 (Cm) 090 (Cm) 0120 (Cm) △10 (Cm) △25 (Cm) △50 (Cm) △75 (Cm) △90 (Cm) △120 (Cm)

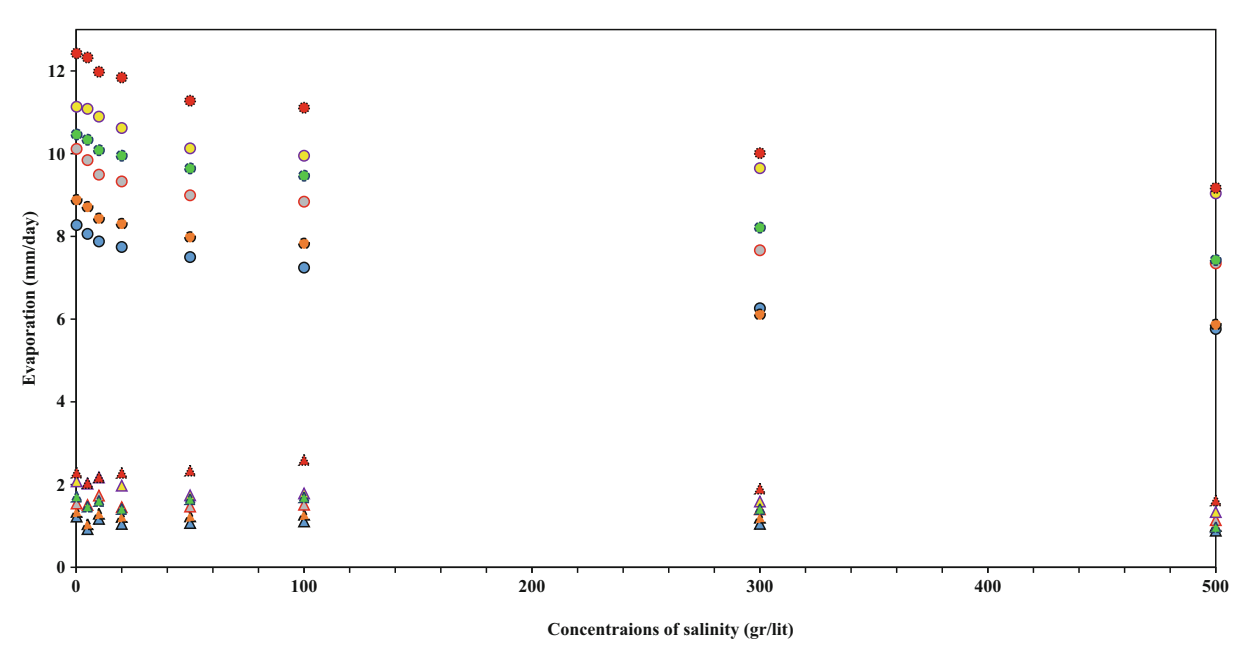


Fig. 5 Evaporation for various concentrations of salinity at each depth

less. It should be noted that as a result of layering, the surface part of the water has the lowest concentration. However, it tends to prevent evaporation compared with freshwater. In general, these will reduce evaporation compared with freshwater.

Figure 7 shows a schematic of barrel layering. The barrels are divided into three layers UCZ (Upper

Convective Zone), NCZ (No-Convective Zone), and LCZ (Low Convective Zone). The first layer has the lowest concentration of salinity, is in contact with the air surface, and the second layer is located below this layer. The second layer acts as insulation for the third layer. The third layer is formed at the lowest depth of the tank and has the highest concentration of

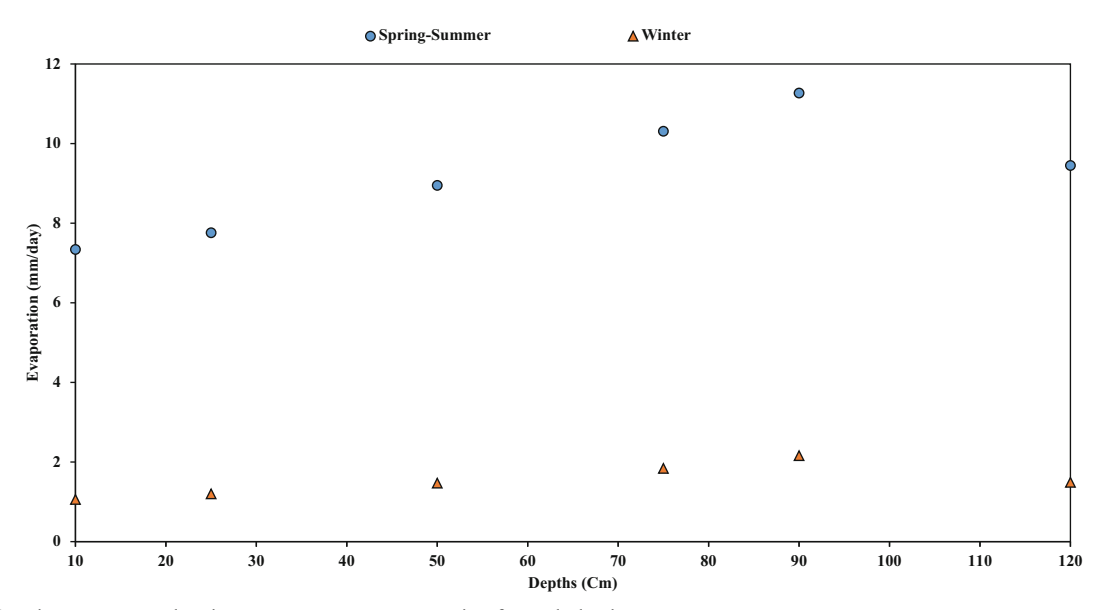


Fig. 6 Winter season and spring-summer season evaporation for each depth

694 Page 14 of 17 Environ Monit Assess (2020) 192:694

 $\textbf{Table 6} \quad \text{The average of surface temperature}(C^{\circ}) \text{ of barrels (winter period)}$

Concentrations of salinity	Depths (cm)				
	120	90	75	50	25	10
500	11.02	12.83	13.90	13.92	14.53	15.29
300	9.87	12.42	13.84	13.90	14.31	14.93
100	9.31	12.58	13.76	13.85	14.26	14.69
50	8.63	12.06	13.65	13.71	14.06	14.64
20	8.52	11.86	13.36	13.38	13.87	14.57
10	8.44	11.45	13.52	13.52	13.69	14.20
5	8.39	11.34	13.41	13.45	13.64	14.13
2	8.19	11.30	13.34	13.40	13.56	14.11

Table 7 The average of bottom temperature(C°) of barrels (winter period)

Concentrations of salinity	Depths (cn	n)				
	120	90	75	50	25	10
500	9.38	11.31	13.02	13.50	19.63	19.77
300	8.71	11.06	12.92	13.10	19.46	19.64
100	8.46	10.99	12.57	12.96	16.46	16.53
50	8.32	10.22	12.25	12.87	15.45	16.42
20	8.24	10.42	11.95	12.59	14.77	16.33
10	8.12	10.31	11.82	12.35	14.54	16.17
5	8.04	9.95	11.73	12.15	14.22	16.02
2	8.04	9.93	11.62	12.09	13.95	15.88

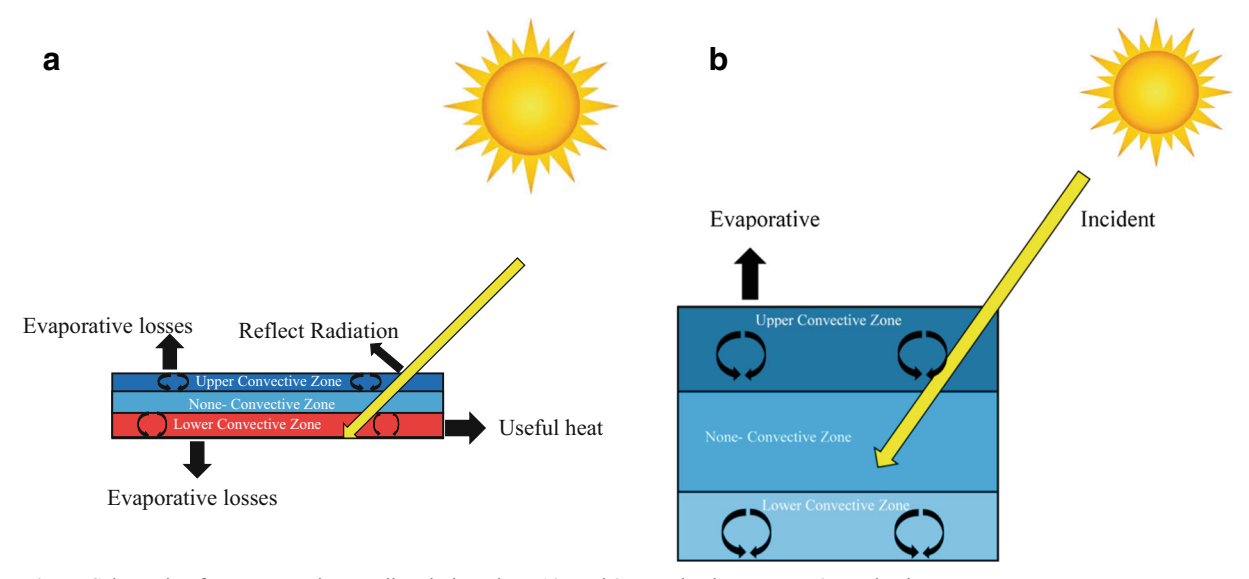


Fig. 7 Schematic of a concentration-gradient in barrels; a 10- and 25-cm depths; b over 50-cm depths



Environ Monit Assess (2020) 192:694 Page 15 of 17 694

Table 8 The average of surface temperature(C°) of barrels (spring-summer period)

Concentrations of salinity	Depth (cm)				
	120	90	75	50	25	10
500	20.1	22.02	22.03	22.96	25.7	26.3
300	19.5	21	21.04	21.91	25.5	26
100	19.3	20.8	20.8	21.32	22.63	24
50	19.3	20.5	20.6	21.11	22.1	23.87
20	19.2	20.5	20.6	20.93	21.9	23.43
10	19.2	20.13	20.13	20.92	21.83	23.31
5	19.2	20.06	20.07	20.9	21.54	22.75
2	19.2	20.06	20.06	20.9	21	22.23

salinity (Biazar et al. 2020c). Also, as the height of the barrels increases, the height of the layers increases.

It should be noted that sunlight will penetrate the initial layers inside the barrel (Giestas et al. 1996; Mansour et al. 2006). In barrels with low height (10 and 25 cm), sunlight passes through the first and second layers and is trapped in the third layer by high concentrations of salinity due to lack of water height, so the temperature is very high (Kurt et al. 2000; Suárez et al. 2010; Ruskowitz et al. 2014.). The temperature of saline water at the bottom of the barrel is very high in tanks with depths of 10 and 25 cm, and this difference is minimized in water with lower concentrations and barrels of similar height, especially in freshwater (Fig. 7 and Tables 6, 7, 8, and 9). As mentioned above, this action is neutralized with increasing depth, and the penetration of sunlight will be up to the initial layers,

so the temperature in the bottom of the barrels will be lower (Rabl and Nielsen 1975; Hull et al. 1988; El-Sebaii et al. 2011)

At low depths, a large amount of energy is reflected for given energy input because there is not enough water mass to absorb energy; this reduces the amount of energy used to evaporate and lowers the evaporation rate. As the depth increases, the water and the absorption of energy increase, a high altitude of water is energized, and the chemical bond between the water molecule and salt molecule becomes weaker, which causes the total amount of evaporation to increase. This process will continue to a certain depth. From depth onward (120 cm), we see a decrease in evaporation rate; however, the 120-cm barrel has more water mass than other barrels. According to Tables 6 and 8, it is observed that the water surface temperature shows a downward trend with

Table 9 The average of bottom temperature(C°) of barrels (spring-summer period)

Concentrations of salinity	Depths (cm))				
	120	90	75	50	25	10
500	18.36	19.71	20.8	22.66	26.97	29
300	18.29	19.43	19.91	21.83	26.49	27.66
100	15.97	19.09	19.31	21.2	23.17	24.37
50	15.77	19.06	19.29	21.06	22.71	24.14
20	15.77	19	19.2	20.86	22.14	23.89
10	15.77	18.86	19.11	20.86	22.11	23.83
5	15.63	18.8	18.94	20.83	21.97	23.49
2	15.6	18.71	18.91	20.83	21.74	23.14



694 Page 16 of 17 Environ Monit Assess (2020) 192:694

increasing the height of the barrels. Also, Fig. 6 has shown an upward trend for the evaporation rate by increasing the height of the barrels. As you know, for the evaporation process to be continuous, it must always be added to the surrounding temperature because the water loses some of its heat as a result of the evaporation process. On the other hand, the vapor pressure also increases with increasing surrounding temperature. Increasing the vapor pressure will also reduce evaporation (Allen et al. 1998; Estévez et al. 2009; Biazar et al. 2019). Therefore, it can be said that the vapor pressure of the barrel surface has improved so much that it has reduced evaporation in the 120-cm barrel.

Conclusion

In this study, 48 barrels were used to derive an equation to estimate evaporation from saline water with different depths and concentrations of salinity (6 depths and 8 different concentrations of salinity). Comparison with the observed values of evaporation values showed that evaporation computed with the derived equation was in a good agreement. At low depth, a large amount of energy received was reflected back, because there was not enough water mass to absorb the energy which caused the amount of energy consumed to become lower for evaporation and reduced the evaporation rate. As the depth increased, the water mass and the energy absorption increased, and a large depth of water was placed under the energy, and the chemical bond between the water molecule and salt molecule was weakened, which increased the amount of evaporation, and the process continued to a certain depth (120 cm). Evaporation rate would start to decrease in this depth. The maximum evaporation rate belonged to 90-cm barrels for the whole period. In saline water, the evaporation value decreased, but the mechanism was identical. The involvement of molecules with cations was higher, and reduced the rate of evaporation in saline water. The maximum evaporation values occurred in summer.

Acknowledgements The authors wish to thank Distinguished Professor John S. Selker (Oregon State University); Professor Reza Delirhasannia (University of Tabriz), Mr. Mohammad Isazadeh and Babak Mohammadpour for help us to complete this study.



References

- Aghelpour, P., Mohammadi, B., & Biazar, S. M. (2019). Long-term monthly average temperature forecasting in some climate types of Iran, using the models SARIMA, SVR, and SVR-FA. *Theoretical and Applied Climatology*, 138(3–4), 1471–1480.
- AL-Khlaifat, A. L. (2008). Dead Sea rate of evaporation. American Journal of Applied Sciences, 5(8), 934–942.
- Allen, R. G., Pereira, L. S., Raes, D., & Smith, M. (1998). Crop evapotranspiration-guidelines for computing crop water requirements-FAO Irrigation and drainage paper 56. Fao, Rome, 300(9), D05109.
- Ashrafzadeh, A., Ghorbani, M. A., Biazar, S. M., & Yaseen, Z. M. (2019). Evaporation process modelling over northern Iran: application of an integrative data-intelligence model with the krill herd optimization algorithm. *Hydrological Sciences Journal*, 64(15), 1843–1856.
- Ashrafzadeh, A., Kişi, O., Aghelpour, P., Biazar, S. M., & Masouleh, M. A. (2020). Comparative study of time series models, support vector machines, and GMDH in forecasting long-term evapotranspiration rates in northern Iran. *Journal* of Irrigation and Drainage Engineering, 146(6), 04020010.
- Ashrafzadeh, A., Malik, A., Jothiprakash, V., Ghorbani, M. A., & Biazar, S. M. (2018). Estimation of daily pan evaporation using neural networks and meta-heuristic approaches. *ISH Journal of Hydraulic Engineering*, 1–9.
- Asmar, B. N., & Ergenzinger, P. (1999). Estimation of evaporation from the Dead Sea. *Hydrological Processes*, 13(17), 2743– 2750.
- Biazar, S. M., Dinpashoh, Y., & Singh, V. P. (2019). Sensitivity analysis of the reference crop evapotranspiration in a humid region. *Environmental Science and Pollution Research*, 26(31), 32517–32544.
- Biazar, S. M., & Ferdosi, F. B. (2020a). An investigation on spatial and temporal trends in frost indices in Northern Iran. *Theoretical and Applied Climatology*. https://doi.org/10.1007/s00704-020-03248-7.
- Biazar, S. M., Rahmani, V., Isazadeh, M., Kisi, O., & Dinpashoh, Y. (2020). New input selection procedure for machine learning methods in estimating daily global solar radiation. *Arabian Journal of Geosciences*, 13, 431.
- Biazar, S. M., Fard, A. F., Singh, V. P., Dinpashoh, Y., & Majnooni-Heris, A. (2020c). Estimation of Evaporation from Saline-Water with More Efficient Input Variables. *Pure and Applied Geophysics*, 1–21.
- Deo, R. C., Ghorbani, M. A., Samadianfard, S., Maraseni, T., Bilgili, M., & Biazar, M. (2018). Multi-layer perceptron hybrid model integrated with the firefly optimizer algorithm for windspeed prediction of target site using a limited set of neighboring reference station data. *Renewable Energy*, 116, 309–323.
- Dinpashoh, Y., Singh, V. P., Biazar, S. M., & Kavehkar, S. (2019). Impact of climate change on streamflow timing (case study: Guilan Province). *Theoretical and Applied Climatology*, 138(1–2), 65–76.
- El-Dessouky, H. T., Ettouney, H. M., Alatiqi, I. M., & Al-Shamari, M. A. (2002). Evaporation rates from fresh and saline water in moving air. *Industrial & Engineering Chemistry Research*, 41(3), 642–650.

Environ Monit Assess (2020) 192:694 Page 17 of 17 694

El-Sebaii, A. A., Ramadan, M. R. I., Aboul-Enein, S., & Khallaf, A. M. (2011). History of the solar ponds: a review study. *Renewable and Sustainable Energy Reviews*, 15(6), 3319– 3325

- Estévez, J., Gavilán, P., & Berengena, J. (2009). Sensitivity analysis of a Penman–Monteith type equation to estimate reference evapotranspiration in southern Spain. *Hydrological Processes: An International Journal*, 23(23), 3342–3353.
- Gianniou, S. K., & Antonopoulos, V. Z. (2007). Evaporation and energy budget in Lake Vegoritis, Greece. *Journal of Hydrology*, 345(3–4), 212–223.
- Giestas, M., Pina, H., & Joyce, A. (1996). The influence of radiation absorption on solar pond stability. *International Journal of Heat and Mass Transfer*, 39(18), 3873–3885.
- Guo, Y., Zhang, Y., Ma, N., Xu, J., & Zhang, T. (2019). Long-term changes in evaporation over Siling Co Lake on the Tibetan Plateau and its impact on recent rapid lake expansion. Atmospheric Research, 216, 141–150.
- Hamdani, I., Assouline, S., Tanny, J., Lensky, I. M., Gertman, I., Mor, Z., & Lensky, N. G. (2018). Seasonal and diurnal evaporation from a deep hypersaline lake: The Dead Sea as a case study. *Journal of Hydrology*, 562, 155–167.
- Hull, J., Nielsen, C. E., & Golding, P. (1989). Salinity gradient solar ponds. Boca Raton, FL: CRC Press.
- Isazadeh, M., Biazar, S. M., & Ashrafzadeh, A. (2017). Support vector machines and feed-forward neural networks for spatial modeling of groundwater qualitative parameters. *Environmental Earth Sciences*, 76(17), 610.
- Khaledian, M. R., Isazadeh, M., Biazar, S. M., & Pham, Q. B. (2020). Simulating Caspian Sea surface water level by artificial neural network and support vector machine models. *Acta Geophysica*, 1–11.
- Kisi, O., Shiri, J., Karimi, S., Shamshirband, S., Motamedi, S., Petković, D., & Hashim, R. (2015). A survey of water level fluctuation predicting in Urmia Lake using support vector machine with firefly algorithm. *Applied Mathematics and Computation*, 270, 731–743.
- Kokya, B. A., & Kokya, T. A. (2008). Proposing a formula for evaporation measurement from salt water resources. *Hydrological Processes: An International Journal*, 22(12), 2005–2012.
- Kurt, H., Halici, F., & Binark, A. (2000). Solar pond conception: Experimental and theoretical studies. *Energ. Convers. Manage.*, 41(9), 939–951.
- Lee, C. H. (1927). Discussion of evaporation on reclamation projects. American Society of Civil Engineers Transactions, 90, 340–343.
- Lide, D. R. (Ed). (2005) CRC handbook of chemistry and physics 86th ed. CRC Publishing: Boca Raton, FL pp 8.
- Lin, S. T., & Sandler, S. I. (1999). Prediction of octanol—water partition coefficients using a group contribution solvation model. *Industrial & Engineering Chemistry Research*, 38(10), 4081–4091.
- Ma, N., Szilagyi, J., Niu, G. Y., Zhang, Y., Zhang, T., Wang, B., & Wu, Y. (2016). Evaporation variability of Nam Co Lake in

- the Tibetan Plateau and its role in recent rapid lake expansion. *Journal of Hydrology*, 537, 27–35.
- Mansour, R. B., Nguyen, C. T., & Galanis, N. (2006). Transient heat and mass transfer and long-term stability of a saltgradient solar pond. *Mechanics research communications*, 33(2), 233–249.
- Mor, Z., Assouline, S., Tanny, J., Lensky, I. M., & Lensky, N. G. (2018). Effect of water surface salinity on evaporation: The case of a diluted buoyant plume over the Dead Sea. *Water Resources Research*, 54(3), 1460–1475.
- Naganna, S. R., Deka, P. C., Ghorbani, M. A., Biazar, S. M., Al-Ansari, N., & Yaseen, Z. M. (2019). Dew point temperature estimation: application of artificial intelligence model integrated with nature-inspired optimization algorithms. *Water*, 11(4), 742.
- Nash, J. E., & Sutcliffe, J. V. (1970). River flow forecasting through conceptual models part I—A discussion of principles. *Journal of hydrology*, 10(3), 282–290.
- Nozari, H., & Azadi, S. (2019). Experimental evaluation of artificial neural network for predicting drainage water and groundwater salinity at various drain depths and spacing. *Neural Computing and Applications*, 31(4), 1227–1236.
- Rabl, A., & Nielsen, C. E. (1975). Solar ponds for space heating. *Solar Energy*, 17(1), 1–12.
- Ruskowitz, J. A., Suárez, F., Tyler, S. W., & Childress, A. E. (2014). Evaporation suppression and solar energy collection in a salt-gradient solar pond. Solar Energy, 99, 36–46.
- Shiri, J., Shamshirband, S., Kisi, O., Karimi, S., Bateni, S. M., Nezhad, S. H. H., & Hashemi, A. (2016). Prediction of waterlevel in the Urmia Lake using the extreme learning machine approach. Water Resources Management, 30(14), 5217– 5229.
- Suárez, F., Tyler, S. W., & Childress, A. E. (2010). A fully coupled, transient double-diffusive convective model for salt-gradient solar ponds. *International Journal of Heat and Mass Transfer*, 53(9-10), 1718–1730.
- Vaheddoost, B., & Kocak, K. (2019). Temporal dynamics of monthly evaporation in Lake Urmia. *Theoretical and Applied Climatology*, 137(3-4), 2451–2462.
- Wang, W., Lee, X., Xiao, W., Liu, S., Schultz, N., Wang, Y., & Zhao, L. (2018). Global lake evaporation accelerated by changes in surface energy allocation in a warmer climate. *Nature Geoscience*, 11(6), 410–414.
- Wurtsbaugh, W. A., Miller, C., Null, S. E., DeRose, R. J., Wilcock, P., Hahnenberger, M., Howe, F., & Moore, J. (2017). Decline of the world's saline lakes. *Nature Geoscience*, 10(11), 816–821.
- Young, A. A. (1947). Some recent evaporation investigations. Transactions American Geophysical Union, 28(2), 279–284.

Publisher's note Springer Nature remains neutral with regard to jurisdictional claims in published maps and institutional affiliations.

